Rabinovich et al, Supplemental material

Supplemental Figure Legends

Figure S1: E75 regulates axon regrowth following axon pruning but not initial outgrowth and may function together with UNF related to Figure 1

(A) Gene structure of *Eip75B* (herein referred to as *E75*), with commonly used nomenclature for each isoform in bold and FlyBase nomenclature below it. Black bars represent coding exons, grey bars represent noncoding exons and lines represent introns. Depicted below are the various mutants we used, dashed lines represent deleted segment, arrow shows P-element insertion. The $E75^{\Delta C}$ deletion was generated via FRT mediated recombination using PBac{RB}e03151 and PBac{RB}Eip75B^{e01229} as parental strains (see Extended Experimental Procedures).

(B) Confocal single slices of MB cell bodies expressing *UAS-E75A-FLAG* (B_1), *UAS-E75B-FLAG* (B_2) and *UAS-E75C-FLAG* (B_3) driven by OK107-Gal4. Inset shows FLAG staining.

(C-H) Confocal Z-projections of WT (C, F) $E75^{\Delta 51}$ (D, G) or $E75^{\Delta C}$ (E, H) MB MARCM neuroblast clones labeled by CD8-GFP driven by 201Y-Gal4 at 3rd instar larva (L3; C-E) or at 24h after puparium formation (APF) (F-H). While $E75^{\Delta 51}$ and $E75^{\Delta C}$ mutants initially extend their γ axons normally (compare D and E to C) at 24h APF they fail to regrow their axons (compare G and H to F). F_2-H_2 show a close up of the medial lobe. In *E75* mutants (G_2 and H_2) the clonal cells (green, outlined in white) have not begun axon regrowth while the heterozygous non-clonal cells (magenta, outlined in blue) regrow normally. Yellow outline marks the α/β axons.

(I-J) Confocal Z-projections of adult MB neuroblast MARCM clones labeled by 201Y-Gal4 driving the expression of membrane bound GFP (CD8-GFP) and *UAS-unf* (I) or additionally *UAS-E75C* (J). *UAS-unf* expression results in a strong pruning defect (I, arrowheads) that is partially repressed by co-expressing E75C (J).

(K) Quantification of regrowth index of *E75* and *unf* epistatic experiments.

Magenta in B is FLAG staining, and in F-J FasII staining. Green is mCD8:GFP driven by OK107-Gal4 (B) or 201Y-Gal4 (F-J). Grey is anti-FLAG (insets in B) or mCD8:GFP driven by 201Y (C-E, F_1-H_1).

Figure S2: Expression of TRiP NOS RNAi decreases anti-NOS and DAF-2 staining in the prothoratic gland and expression of both NOS RNAi lines, IR-X and TRiP, in MB neurons promote regrowth *ex vivo*, related to Figure 2.

(A-B) Single slices of the prothoracic gland (PG) of WT (A) or with NOS RNAi (TRiP) expressed by the PG specific driver amn-Gal4 (B) stained with an antibody for NOS (Lacin et al., 2014) (A_1, B_1) or with the NO sensor DAF-2 (A_2, B_2). Expressing TRiP NOS RNAi in the PG decreases both anti-NOS staining and NO levels, validating this new RNAi line.

(C-G) Confocal Z-projections of brains dissected at 23h APF and cultured for 22h *ex vivo*, expressing TRiP NOS RNAi (C-D) or IR-X NOS-RNAi (E-G) driven by repo-Gal4 (C, E), c155-Gal4 (D, F) or OK107-Gal4 additionally driving expression of CD8-GFP (G). Lower panels show a subset of slices of the medial lobe stained against FasII using a thermal lookup table with the γ lobe demarcated in red and the α/β lobe in black.

(H) Quantification of developmental regrowth of the genotypes shown in Figure 2B, 2D, 2H and panels C-D. *** p<0.001; *p<0.05 One-way ANOVA was performed with a Dunnett's post-hoc test.

Grey is guinea pig anti-NOS staining (A_1 and B_1) or DAF-2 staining (A_2 and B_2).

Grey in C-F, magenta in G and thermal look-up table represent FasII staining, green in G is OK107 driven mCD8:GFP.

Figure S3: Additional analysis of NOS RNAi (TRiP) and expression of an additional NOS RNAi line (IR-X) also causes precocious regrowth *in vivo*, related to Figure 3.

(A-D) Confocal Z-projections of brains dissected at 24h APF containing NOS RNAi alone (A), expressing NOS RNAi^{TRiP} (B-C) or expressing NOS RNAi^{IR-X} (D-F) driven by repo-Gal4 (B,D), c155-Gal4 (C,E) or OK107-Gal4 (F). Lower panels show a subset of slices of the medial lobe stained against FasII using a thermal lookup table (A-E) or magnified medial lobe of GFP driven by OK107-Gal4 (F) with the γ lobe demarcated in red and the β lobe in black.

Grey and magenta represents FasII staining. Green in F is OK107 driven mCD8:GFP.

Figure S4: The repression of regrowth by NO is not mediated by the canonical sGC pathway and S6K^{CA} can bypass DETA inhibition, related to Figure 4.

(A-D) Confocal Z-projections of brains expressing CD8-GFP driven by 201Y-Gal4, dissected at 23h APF and cultured *ex vivo* for 22h, untreated (A), or treated with the soluble guanylyl cyclase (sGC) inhibitor ODQ (B), the NOS inhibitor L-NAME (C), L-NAME with the cGMP analog 8-bromo-cGMP (D). ODQ does not affect axon regrowth (B) and 8-bromo-cGMP does not suppress the growth promoting effect of L-NAME (D), suggesting that NOS does not function through the sGC pathway.

(E-F) Confocal Z-projections of WT (H) or *dgcα1^{207}* mutant (I) brains at 24h APF stained for FasII. Brains mutant for the α subunit of sGC do not show precocious regrowth at 24h APF indicating that NO does not function via this pathway. Lower panels show a subset of slices of the medial lobe stained against FasII using a thermal lookup table with the γ lobe demarcated in red and the α/β lobe in black.

(G) Model of the canonical soluble guanylate cyclase (sGC) pathway. ODQ is a competitive inhibitor of NO binding to heme bound to sGC.

(H-I) Confocal Z-projections of brains expressing CD8-GFP driven by 201Y-Gal4, dissected at 23h APF and cultured *ex vivo* for 22h treated with the NO donor DETA (H) or DETA but additionally expressing the constitutively active form of S6 kinase (S6K^{CA}; I). Overexpression of S6K^{CA} promotes regrowth even in the presence of DETA (I), suggesting that the TOR pathway functions downstream of NO signaling in MB remodeling.

Green is mCD8:GFP driven by 201Y, magenta and grey is FasII staining.

Figure S5: Pruning defect of NOS RNAi expressing brains and time course analysis of R82G02-Gal4, R82G02:mtdT-3XHA and R71G10-Gal4 – related to Figure 5

(A-D) Confocal Z-projections of the MB dorsal lobes in WT (A), NOS RNAi expressed by repo-Gal4 (B), c155-Gal4 (C) or OK107-Gal4 (D) brains stained with FasII. Arrowheads mark unpruned larval γ axons.

(E-F) Confocal Z-projections of MB neurons at 24h APF expressing NOS RNAi driven by repo-Gal4 (E) or c155-Gal4 (F) and the Gal4 independent MB marker R82G02:mtdT-3XHA

(G-O) Confocal Z-projections of MB neurons at 6h APF (G, J, M), 24h APF (H, K, N) or adult (I, L, O) expressing CD8:GFP driven by R82G02-Gal4 (G-I) or R71G10-Gal4 (M-O) or the expressing the Gal4 independent MB marker R82G02:mtdT-3XHA (J-L).

Magenta in G-O and grey in A-D represents FasII staining. Grey in E-F is anti-HA and in P-R is mCD8:GFP driven by 201Y-Gal4. Green is mCD8:GFP driven by R82G02-Gal4 (G-I), or R71G10-Gal4 (M-O), or anti-HA (J-L)

Figure S6: Analysis of three dNOS allele combinations display both pruning and regrowth phenotypes, and analysis of new CRISPR alleles – relates to Figure 5

(A-J) Confocal Z-projections of brains dissected at 24h APF of $dNOS^{\Delta 15}$ heterozygotes (A), $dNOS^{\Delta 15}$ homozygous brains (B), $dNOS^{\Delta 15}/dNOS^{C}$ transheterozygotes (C-D), $dNOS^{1}$ heterozygotes (E), $dNOS^{\Delta 15}/dNOS^{1}$ transheterozygotes (F-G), $dNOS^{C}$ heterozygotes (H) and $dNOS^{1}/dNOS^{C}$ transheterozygotes (I-J). Lower panels show a subset of slices of the medial lobe stained against FasII using a thermal lookup table with the γ lobe demarcated in red and the α/β lobe in black. Similar to what is seen with NOS RNAi as well as homozygous mutant brains, transheterozygous brains using 3 independent dNOS alleles show a pruning defect (arrowheads in B, D, G, J) and enhanced regrowth (B, C, F, I).

(K) PCR of CRISPR mutants to verify deletions. Whole body DNA extract from y,w flies (1st group), $dNOS^{\Delta All}$ (2nd group) or $dNOS^{\Delta N\text{-}ter}$ (3rd group) homozygous animals. Schematic representation of the primers location is depicted in the diagram below. See Extended Experimental Procedures for precise primer sequences and expected product sizes.

(L) RT-PCR of RNA extracted from $dNOS^{\Delta All}$ (lane 1), $dNOS^{\Delta N\text{-}ter}$ (lane 2), $dNOS^{\Delta 15}$ (lane 3) or WT (lane 4) brains. Product using primers encompassing exons 3 and 4 (lower panel) show that it is not expressed in any of the mutants. Product using primers for NOS exons 10-11 (see Figure S7 for NOS primer location) is not detected in either $dNOS^{\Delta All}$ or $dNOS^{\Delta 15}$ but is present in $dNOS^{\Delta N\text{-}ter}$.

(M-O) Confocal Z-projections of WT (M), $dNOS^{\Delta All}$ (N) or $dNOS^{\Delta N\text{-}ter}$ (O) MB MARCM neuroblast clones labeled by CD8-GFP driven by 201Y-Gal4 at 24h APF. MARCM clones of *dNOS* mutants do not display pruning and regrowth phenotypes unlike whole animal mutants, indicating that NOS does not function in a cell autonomous manner.

Grey in A-J and thermal look-up table represents FasII staining. Grey in M-O is mCD8:GFP driven by 201Y-Gal4

Figure S7: Calmodulin RNAi decreases NO levels and phenocopies NOS knockdown, annotation of *dNOS* locus with short RNA isoforms and localization of primers, relates to Figure 7

(A-B) Confocal single slices of the prothoracic gland (PG) of WT (A) or with Cam RNAi (TRiP) expressed by the PG specific driver amn-Gal4 (B) stained using the NO fluorescent indicator DAF-2.

(C-E) Confocal Z-projections of brains dissected at 24h APF of WT (C) or of brains expressing Cam-RNAi driven by OK107-Gal4 (D-E). Knocking down Cam in the MB resulted in enhanced regrowth (D) and a pruning defect (arrowhead in E), see Table S1 for more analyses. Lower panels show a subset of slices of the medial lobe stained against FasII using a thermal lookup table with the γ lobe demarcated in red and the α/β lobe in black.

(F-G) Quantification of the regrowth (F) and pruning (G) phenotypes in D-E. ***p<0.001

(H) Schematic representation of *dNOS* genomic locus. Black bars represent coding exons, grey bars represent noncoding exons and lines represent introns. Full length active *dNOS1* is shown as transcript RA with two additional short transcripts we have verified as being expressed in the MB. NOS common primers amplify a section encompassing exons 10-11 (red) and NOS exon 3-4 (blue) that are both shared for all transcripts. RB primers use an untranslated exon that is located upstream of the RA 5' exon (green). RD primers include an exon-exon junction that is unique for the RD isoform (orange). For primer sequence refer to the Extended Experimental Procedures.

(I) (Graph summarizing effects of $dNOS^{\Delta 15}$ with and without expression UAS-dNOS. While $dNOS^{\Delta 15}$ alone or UAS-dNOS alone are viable, combining the two results in early pupal lethality. Percentage was calculated as the amount of flies observed divided by the expected number of flies as a result of a cross using Mendelian genetic probabilities.

Rabinovich et al, Supplemental material

Supplemental Experimental Procedures

Construction of transgenes and transgenic flies

Detailed maps of the plasmids constructed will be supplied upon request.

For UAS-E75: E75A and E75B coding sequences were amplified from pMT-TAP E75A (provided by H. Krause) and pGEM-E75B (provided by C. Thummel), respectively. As we were unable to isolate the E75C transcript from cDNA based on the annotated transcripts, we used the 5'Race kit GeneRacer (Invitrogen) to identify the genuine transcription start site. The transcription start site is located 1152bp downstream of the annotated start site. We therefore amplified E75C cDNA using the following primers: (5') ATGCACCATCAGCAGCAACAGCAA and (3') TTACGCCTCCAGCATTAC. All transcripts were cloned into pDONR201 (Invitrogen) and then inserted into pTWF-AttB (Yaniv et al., 2012) and injected into the attP40 landing site using φC31 integration (BestGene).

For 82G02:mtdT-3XHA The Gal4 sequence in pBPGUw plasmid was excised using KpnI and HindIII and replaced with mtdT-3XHA sequences that were amplified from pUASTattB-mtdT-3XHA to give rise to what we named pBPTHUw. The DNA sequences that drive Gal4 expression in R82G02 flies was isolated using the primer sequence provided by Janelia Farm (http://flweb.janelia.org/cgi-bin/flew.cgi) and cloned into pBPTHUw using the Gateway system. This construct was injected into attP2 landing site using φC31 integration (BestGene).

For UAS-dNOS (UAS-dNOS^{OS}): The full length dNOS cDNA was amplified using the primers 5'-ATGTCGCAGCATT 3'- CGAATGGCCTCCCAGCCATAA and cloned into pDONR221. To allow for optimal transgene expression and site specific integration we generated a modified Gateway destination vector based on pDESTp10aw (Shearin et al., 2013) to which we added 10XUAS-IVS-Syn21 (from pJFRC81; Pfeiffer et al., 2012) upstream to the gateway cassette to generate a plasmid that we named: pDEST-UAS-IVS-Syn21-p10aw. The resulting optimized dNOS transgene was injected into the 86Fb landing site using φC31 integration (BestGene).

E75$^{\Delta C}$ was constructed with FLP-FRT mediated deletion (Parks et al., 2004) using PBac{RB}e03151 and PBac{RB}Eip75B^{e01229} as parental strains. Tested deletions were recombined to FRT2A containing chromosomes.

For cell culture experiments pA-UNF-Flag and pA-E75C-HA were constructed by performing a Gateway LR reaction of the entry vectors pENTR-UNF (Yaniv et al, 2012) or pDONR-E75C (see above) into either pAWF or pAWH (Gateway).

Construction of CRISPR mutant flies

Guide RNA sequences were cloned into pCFD4 using Gibson assembly (NEB) as described by Port et al (2014). The primers used for generating *dNOS$^{\Delta all}$* (see Figure 5):

5'-TATATAGGAAAGATATCCGGGTGAACTTCTCGAAGTAATCAAAATAGGAGTTTTAGAGCTAGAAATAGCAAG-3'

5'-ATTTTAACTTGCTATTTCTAGCTCTAAAACACAGGTGAACCACTTGGACAGACGTTAAATTGAAAATAGGTC-3'

The primers used for generating *dNOS$^{\Delta N\text{-}ter}$*(see Figure 5):

5'-TATATAGGAAAGATATCCGGGTGAACTTCCAAATAATCTACTCGCTACGGTTTTAGAGCTAGAAATAGCAAG-3'

5'-ATTTTAACTTGCTATTTCTAGCTCTAAAACACAGGTGAACCACTTGGACAGACGTTAAATTG AAAATAGGTC-3'

pCFD4 plasmid was injected into attP40 landing site using φC31 integration (BestGene). Resulting flies were crossed with nanos-Cas9 flies (Bloomington stock #54591). Two generations later single males were isolated and checked for deletion using specific primers.

For all PCR reactions the forward primer (P1) was: 5'-CTGCCGATTTTGCTCATTAAAC-3'

For *dNOS*$^{\Delta all}$ the reverse primer (P4) was: 5'-GCAATTAAATATTGTCGCTTTGT-3' and the expected products were: deletion product ~400bp, no deletion 18kb

For *dNOS*$^{\Delta N\text{-}ter}$ the reverse primer (P3) was: 5'-GCACATTAGAATGCAAAGCG-3' and the expected products were: deletion product ~400bp, no deletion 9kb.

The control reverse primer (P2) was: 5'-CAGCAACAGCAACTGCAGCA-3' resulting in a product of ~400bp in the case of an intact locus and no product in the case of a deletion.

In *dNOS*$^{\Delta all}$ 27,529 bp were deleted, in *dNOS*$^{\Delta N\text{-}ter}$ 8,595 bp were deleted

Cell culture and transfection

Drosophila BG3 cells were maintained in Schneider's medium supplemented with 10% FCS, 10µg/ml insulin and antibiotics and grown at 25°C. Cell were transfected with pA-UNF-Flag and/or pA-E75C-HA using calcium phosphate transfection. ~85 hours following transfection cells were treated with 100µM of the NO scavenger PTIO (Sigma Aldrich) for 5 hours before cells were harvested.

Co-immunprecipitation

Nuclear extracts were extracted from transfected BG3 cells using the Nuclear Complex Co-IP kit (Active Motif) according to manufacture's instructions. Nuclear extracts were incubated with anti-Flag M2 Affinity Gel (Sigma Aldrich) that was washed twice in TBS, and twice in low IP buffer (Active Motif) overnight at 4°C. The following morning, beads were pelleted, washed twice with low IP buffer supplemented with 1mg/ml BSA, twice with low IP buffer without BSA and with lysis buffer (50mM Tris HCL pH 7.4, 150mM NaCl, 1mM EDTA, 1% Triton X-100, protease inhibitors) three times (two rinses plus one 30' wash at 4°C). Beads were then washed twice with TBS. Bound Flag proteins were eluted with 150ng/µl 3XFLAG peptide (Sigma Aldrich) rotating for 40' at 4°C. Immunoprecipitates and input were run on 8% SDS-PAGE gel followed by western blot analysis. Primary antibodies used were mouse M2 anti-Flag (Sigma Aldrich) and rat anti-HA (Roche). Secondary antibodies used were anti-mouse HRP and anti-rat HRP (Jackson Laboratories). Blots were visualized using BioRad ChemiDoc XRS+ apparatus.

Quantification and statistical analyses

For the quantification of developmental regrowth in MARCM clones (Figures 1, 4 and 7), we used a method previously described (Yaniv et al, 2012). In short, we determined the γ lobe occupancy by comparing the clonal (GFP) vs non clonal (FasII staining) in the Z-plane cross section. To calculate the regrowth index, we then divided the lobe occupancy of the clonal axons at a distal section by a proximal section. Statistical analysis was performed by a one-way ANOVA including all groups followed by a Dunnett's T3 post-hoc test. Significance was calculated as $p<0.05$.

For quantification of regrowth and pruning in Figure 2 and 4 we used GFP staining and in Figures 3, 5, 6 and S7), FasII staining was used. Confocal lsm stacks were given to an independent lab member who blindly ranked the severity of the pruning defect or the extent of the adult γ lobe regrowth. For NOS RNAi analysis one-way ANOVA was performed using 4 groups: WT, OK107-, c155- and repo-Gal4 driving the RNAi transgene followed by a Dunnett's post-hoc test. For Cam RNAi a two-tailed T-test was performed between WT and OK107-Gal4 driving RNAi expression. For $S6K^{CA}$ a one tailed T-test was performed between WT and 201Y-Gal4 driving $S6K^{CA}$ expression. Significance was calculated as $p<0.05$.

For quantifying pruning efficacy in *ex vivo* cultured brains (Figure 6D, H): Pruning index was calculated as the intensity of GFP at the dorsal tip/intensity of GFP at the peduncle. An index of 1 demonstrates no pruning and 0 demonstrates complete pruning. For more details see Rabinovich et al, 2015.

For quantifying the effect of overexpressing UAS-NOS (Figure 6K), the number of "holes" in FasII staining at the dorsal tip and in the peduncle were blindly counted by looking at lsm stacks. A two-tailed T-test was performed between WT and OK107-Gal4 driving UAS-NOS expression. Significance was calculated as $p<0.05$.

DAR-4M intensities (Figure 7) were quantified using the Imaris program (Bitplane). An automatic segmentation protocol was carried out using the "Surfaces" algorithm. In short, GFP fluorescence in images of MB cell bodies was used for segmentation, and the average fluorescence of DAR-4M within the MB cell bodies was quantified. Analysis of all samples was conducted under the same imaging conditions, including mounting, laser intensities and magnifications. A two-tailed T-test was performed between 6h APF and 24h APF. Significance was calculated as $p<0.05$.

Cell isolation and cDNA amplification

Brains were dissected in Ringer's solution and incubated with 2mg/ml collagenase/dispase mix (Roche) in cell dissociation solution (Sigma-Aldrich) for 15 minutes at 29ºC, followed by washing with dissociation solution. Brains were mechanically dissociated into single cells and transferred via 37µm mesh.

Sorting of 1,000 cells was done using a 100µm nozzle and low pressure in BD FACSAria Fusion cell sorter directly into PicoPure RNA Isolation Kit extraction buffer (Life Technologies) followed by RNA extraction using the kit. The RT-PCR and pre-amplification steps have been previously described (Jaitin et al., 2014) with some modifications. Briefly, SuperScript III + Platinum Taq DNA Polymerase One-Step RT-PCR System (Life Technologies) were used for reverse transcription + 12 cycles of pre-amplification using a mix of transcript specific primers (see below) in concentration of 50nM each. Following RT and pre-amplification, the samples were treated by Exonuclase I (NEB) and then subjected to the second PCR using the Phusion High-Fidelity DNA Polymerase (Thermo).

For whole brain RT-PCR comparison (Figure 7E and S6K) brains were dissociated as described above and RNA directly extracted followed by one step RT-PCR + amplification with transcript specific primers (see below) using the SuperScript III + Platinum Taq DNA Polymerase One-Step RT-PCR System kit.

Due to lack of known function, annotation of the *dNOS* locus in FlyBase does not include all of the isoforms proposed by Stasiv and colleagues. Therefore, we based our analyses on an old annotation that was available in RefSeq and also at archived FlyBase annotation (http://fb2012_06.flybase.org/reports/FBgn0011676.html).

Rabinovich et al, Supplemental material

Primers used for both cDNA reverse transcription and PCR:

RPS3 1st set: 5'- ACGCAAGTTCGTTTCCGATG -3' and 5'- GATGATCTCAGTGCGAGAGGG -3'
RPS3 2nd set: 5'-CTTTTCTGCGCACCACGTTT-3' and 5'-GCCATCGGAAACGAACTTGC-3'
NOS common 5'-TCGAGAACGAGTCCAAGCTC-3' and 5'-GGAATACCGGCGTTATGGA-3'
NOS RD transcript 5'-GTGCCGGCAGATTCTTTCC-3' and 5'-AGGAAGTCCTTGGCGTGTTC-3'
NOS RB transcript 5'-AATATGCACGACATTTTGAAGCA-3' and 5'-ACAGGTGAACCACTTGGACA-5'

Drosophila Genotypes

hsFLP is y,w,hsFLP122; CD8 is UAS-mCD8::GFP; 19A, G13, 40A and 2A are FRTs on X, 2R, 2L and 3L respectively; Gal80 is TubP-Gal80, NOS-RNAi^{TRiP} is UAS-NOS TRiP line (#50675) and NOS-RNAi^{IRX} is UAS-NOS IR-X line (Caceres, et al. 2011). Males and females were used interchangeably but only the female genotype is mentioned.

Figure 1:

(B) hsFLP, CD8/+;201Y-Gal4, CD8/+; 2A/ Gal80, 2A
(C) hsFLP, CD8/+;201Y-Gal4, CD8/+; *E75*$^{\Delta 51}$, 2A/ Gal80, 2A
(D) hsFLP, CD8/+;201Y-Gal4, CD8/UAS-E75A-FLAG; *E75*$^{\Delta 51}$, 2A/ Gal80, 2A
(E) hsFLP, CD8/+;201Y-Gal4, CD8/UAS-E75B-FLAG; *E75*$^{\Delta 51}$, 2A/ Gal80, 2A
(F) hsFLP, CD8/+;201Y-Gal4, CD8/UAS-E75C-FLAG; *E75*$^{\Delta 51}$, 2A/ Gal80, 2A
(G) hsFLP, CD8/+;201Y-Gal4, CD8/+; *E75*^{A81}, 2A/ Gal80, 2A
(H) hsFLP, CD8/+;201Y-Gal4, CD8/+; *E75*^{07041}, 2A/ Gal80, 2A
(I) hsFLP, CD8/+;201Y-Gal4, CD8/+; *E75*$^{\Delta C}$, 2A/ Gal80, 2A
(J) hsFLP, CD8/+;201Y-Gal4, CD8/UAS-E75C-FLAG; *E75*$^{\Delta C}$, 2A/ Gal80, 2A
(K) hsFLP, CD8/+;201Y-Gal4, CD8/UAS-Rheb; *E75*$^{\Delta 51}$, 2A/ Gal80, 2A
(L) hsFLP, CD8/+;201Y-Gal4, CD8/UAS-S6K.STDE; *E75*$^{\Delta 51}$, 2A/ Gal80, 2A

Figure 2:

(B-G) 201Y-Gal4/+; 10XUAS-IVS-mCD8::GFP/+
(H) CD8/+;OK107-Gal4/+
(I-J) CD8/+; NOS-RNAi^{TRiP}/+; OK107-Gal4/+

Figure 3:

(A) NOS-RNAi^{TRiP}/+
(B) CD8/+; NOS-RNAi^{TRiP} /+; OK107-Gal4/+

Figure 4:

(A-B) hsFLP, CD8/+; 40A/ Gal80, 40A, CD8, 201Y-Gal4
(D) hsFLP, CD8/+;201Y-Gal4, CD8/+; *E75*$^{\Delta 51}$, 2A/ Gal80, 2A
(E) hsFLP, CD8/+;G13, 201Y-Gal4, *unf*^{LL04325}, CD8/ G13, Gal80
(F) hsFLP, CD8/+; *TOR*^{LL04239}, 40A / Gal80, 40A, CD8, 201Y-Gal4
(G) 201Y-Gal4/+; 10XUAS-IVS-mCD8::GFP/+
(H) 201Y-Gal4/+; 10XUAS-IVS-mCD8::GFP/+;UAS-S6K.STDE/+

Figure 5:

(B) GMR82G02:mtdT-3XHA/+
(C) GMR82G02:mtdT-3XHA/+; NOS-RNAi^{TRiP}/+; OK107-Gal4/+

(D) 10XUAS-IVS-mCD8::GFP/+; GMR71G10-Gal4/+
(E) 10XUAS-IVS-mCD8::GFP/+; NOS-RNAi^{TRiP}/GMR71G10-Gal4
(G) y,w
(H-I) *dNOS*$^{\Delta All}$, 40A / *dNOS*$^{\Delta N\text{-}ter}$, 40A

Figure 6:

(A-C, E-F) 201Y-Gal4/+; 10XUAS-IVS-mCD8::GFP/+
(G) 201Y-Gal4/UAS-macNOS; 10XUAS-IVS-mCD8::GFP/+
(I) CD8/+; OK107-Gal4/+
(J) CD8/UAS-macNOS; OK107-Gal4/+

Figure 7:

(A-B) CD8/+; 201Y-Gal4/+
(G) hsFLP, CD8/+; 40A / Gal80, 40A; R71G10-Gal4/+
(H) hsFLP, CD8/+; 40A/ Gal80, 40A; UAS-dNOS^{OS}/R71G10-Gal4
(I) hsFLP, CD8/+; *dNOS*$^{\Delta N\text{-}ter}$, 40A / Gal80, 40A; R71G10-Gal4/+
(J) hsFLP, CD8/+; *dNOS*$^{\Delta N\text{-}ter}$, 40A / Gal80, 40A; UAS-dNOS^{OS}/R71G10-Gal4

Figure S1:

(B_1) UAS-E75A-FLAG/CD8; OK107-Gal4/+
(B_2) UAS-E75B-FLAG/CD8; OK107-Gal4/+
(B_3) UAS-E75C-FLAG/CD8; OK107-Gal4/+
(C, F) hsFLP, CD8/+; 201Y-Gal4, CD8/+; 2A/ Gal80, 2A
(D, G) hsFLP, CD8/+; 201Y-Gal4, CD8/+; *E75*$^{\Delta 51}$, 2A/ Gal80, 2A
(E, H) hsFLP, CD8/+; 201Y-Gal4, CD8/+; *E75*$^{\Delta C}$, 2A/ Gal80, 2A
(I) hsFLP, CD8/+; 40A/ Gal80, 40A, 201Y-Gal4, CD8/; UAS-unf-FLAG /+
(J) hsFLP, 19A, G80/hsFlp,19A; UAS-E75C-FLAG/201Y-Gal4, CD8; UAS-unf-FLAG/+

Figure S2:

(A) Amn-Gal4/+
(B) NOS-RNAi^{TRiP}/+; Amn-Gal4/+
(C) NOS-RNAi^{TRiP}/ repo-Gal4
(D) c155-Gal4/+; NOS-RNAi^{TRiP}
(E) NOS-RNAi^{IRX}/ repo-Gal4
(F) c155-Gal4/+; NOS-RNAi^{IRX}
(G) CD8/+; NOS-RNAi^{IRX} /+; OK107-Gal4/+

Figure S3:

(A) NOS-RNAi^{TRiP} /+
(B) NOS-RNAi^{TRiP} / repo-Gal4
(C) c155-Gal4/+; NOS-RNAi^{TRiP}
(D) NOS-RNAi^{IRX} / repo-Gal4
(E) c155-Gal4/+; NOS-RNAi^{IRX}
(F) CD8/+; NOS-RNAi^{IRX} /+; OK107-Gal4/+

Figure S4:

(A-E, H) 201Y-Gal4/+; 10XUAS-IVS-mCD8::GFP/+
(F) dgcα1^{207}
(I) 201Y-Gal4, CD8; UAS-S6K.STDE/+

Figure S5:

(A) NOS-RNAi^{TRiP} /+
(B) NOS-RNAi^{TRiP}/ repo-Gal4
(C) c155-Gal4/+; NOS-RNAi^{TRiP}
(D) CD8/+; NOS-RNAi^{TRiP}/+; OK107-Gal4/+
(E) GMR82G02:MtdT-3XHA/+; NOS-RNAi^{TRiP}/ repo-Gal4
(F) c155-Gal4/ +; GMR82G02:mtdT-3XHA/+ ; NOS-RNAi^{TRiP}/+
(G-I) 10XUAS-IVS-mCD8::GFP/+; GMR82G02-Gal4/+
(J-L) GMR82G02:mtdT-3XHA/+
(M-O) 10XUAS-IVS-mCD8::GFP/+; GMR71G10-Gal4/+

Figure S6

(A) *dNOS*$^{\Delta 15}$/+
(B) *dNOS*$^{\Delta 15}$/*dNOS*$^{\Delta 15}$
(C-D) *dNOS*$^{\Delta 15}$/ *dNOS*^{C}
(E) *dNOS*^{1}/+
(F-G) *dNOS*$^{\Delta 15}$/*dNOS*^{1}
(H) *dNOS*^{C}/+
(I-J) *dNOS*^{1}/*dNOS*^{C}
(M) hsFLP, CD8/+; 40A/ Gal80, 40A, 201Y-Gal4, CD8
(N) hsFLP/+; *NOS*$^{\Delta All}$, 40A/ Gal80, 40A, 201Y-Gal4, CD8
(O) hsFLP/+; *NOS*$^{\Delta N\text{-}ter}$, 40A/ Gal80, 40A, 201Y-Gal4, CD8

Figure S7

(A) Amn-Gal4/+
(B) UAS-Cam-RNAi/ Amn-Gal4
(C) CD8/+; OK107-Gal4/+
(D-E) CD8/+; UAS-Cam-RNAi/+; OK107-Gal4/+

Table S1:
pertubations various the in defects regrowth and pruning the of summary A
Related to Figure 5.

Genotype	WT	Pruning defect only	Precocious regrowth only	Both phenotypes
OK107	13/13 (100%)	0/13 (0%)	0/13 (0%)	0/13 (0%)
OK107>*NOS* RNAi	1/25 (4%)	15/25 (60%)	2/25 (8%)	7/25 (28%)
OK107>*Cam* RNAi	7/23 (30%)	8/23 (35%)	2/23 (9%)	6/23 (26%)
$dNOS^{\Delta 15}$	5/25 (20%)	8/25 (32%)	5/25 (20%)	2/25 (8%)
$dNOS^{\Delta 15}/dNOS^{C}$	2/14 (14%)	3/14 (22%)	7/11 (50%)	2/14 (14%)
$dNOS^{\Delta 15}/dNOS^{1}$	3/22 (14%)	2/22 (9%)	12/22 (54%)	5/22 (23%)
$dNOS^{C}/dNOS^{1}$	2/16 (16%)	3/12 (25%)	5/12 (42%)	2/12 (16%)
$dNOS^{\Delta all}$	5/22 (23%)	6/22 (27%)	9/22 (41%)	2/21 (9%)
$dNOS^{\Delta N\text{-}ter}$	3/13 (23%)	3/13 (23%)	6/13 (46%)	1/13 (7%)
$dNOS^{\Delta all}/dNOS^{\Delta N\text{-}ter}$	9/21 (43%)	7/21 (33%)	3/21 (14%)	2/21 (9%)

Table S2:
γ lobe occupancy at 30h APF is not significantly affected by overexpression of NOS transgenes, related to Figure 7

30h APF	Full γ lobe	Partial regrowth	No regrowth
Control	6/7 (86%)	1/7 (14%)	0/17 (0%)
OK107>UAS-dNOS^{GE}	10/11 (91%)	1/11 (9%)	0/11 (0%)
OK107>UAS-dNOS^{OS}	8/14 (57%)	6/14 (43%)	0/14 (0%)
OK107>UAS-dNOS^{GE} +UAS-Cam	8/10 (80%)	2/10 (20%)	0/10 (0%)

Supplemental references

Jaitin, D.A., Kenigsberg, E., Keren-Shaul, H., Elefant, N., Paul, F., Zaretsky, I., Mildner, A., Cohen, N., Jung, S., Tanay, A.*, et al.* (2014). Massively parallel single-cell RNA-seq for marker-free decomposition of tissues into cell types. Science *343*, 776-779.

Parks, A.L., Cook, K.R., Belvin, M., Dompe, N.A., Fawcett, R., Huppert, K., Tan, L.R., Winter, C.G., Bogart, K.P., Deal, J.E.*, et al.* (2004). Systematic generation of high-resolution deletion coverage of the Drosophila melanogaster genome. Nature genetics *36*, 288-292.

Pfeiffer, B.D., Truman, J.W., and Rubin, G.M. (2012). Using translational enhancers to increase transgene expression in Drosophila. Proc Natl Acad Sci U S A *109*, 6626-6631.

Port, F., Chen, H.M., Lee, T., and Bullock, S.L. (2014). Optimized CRISPR/Cas tools for efficient germline and somatic genome engineering in Drosophila. Proc Natl Acad Sci U S A *111*, E2967-2976.

Shearin, H.K., Dvarishkis, A.R., Kozeluh, C.D., and Stowers, R.S. (2013). Expansion of the gateway multisite recombination cloning toolkit. PLoS One *8*, e77724.

Rabinovich et al Figure S1

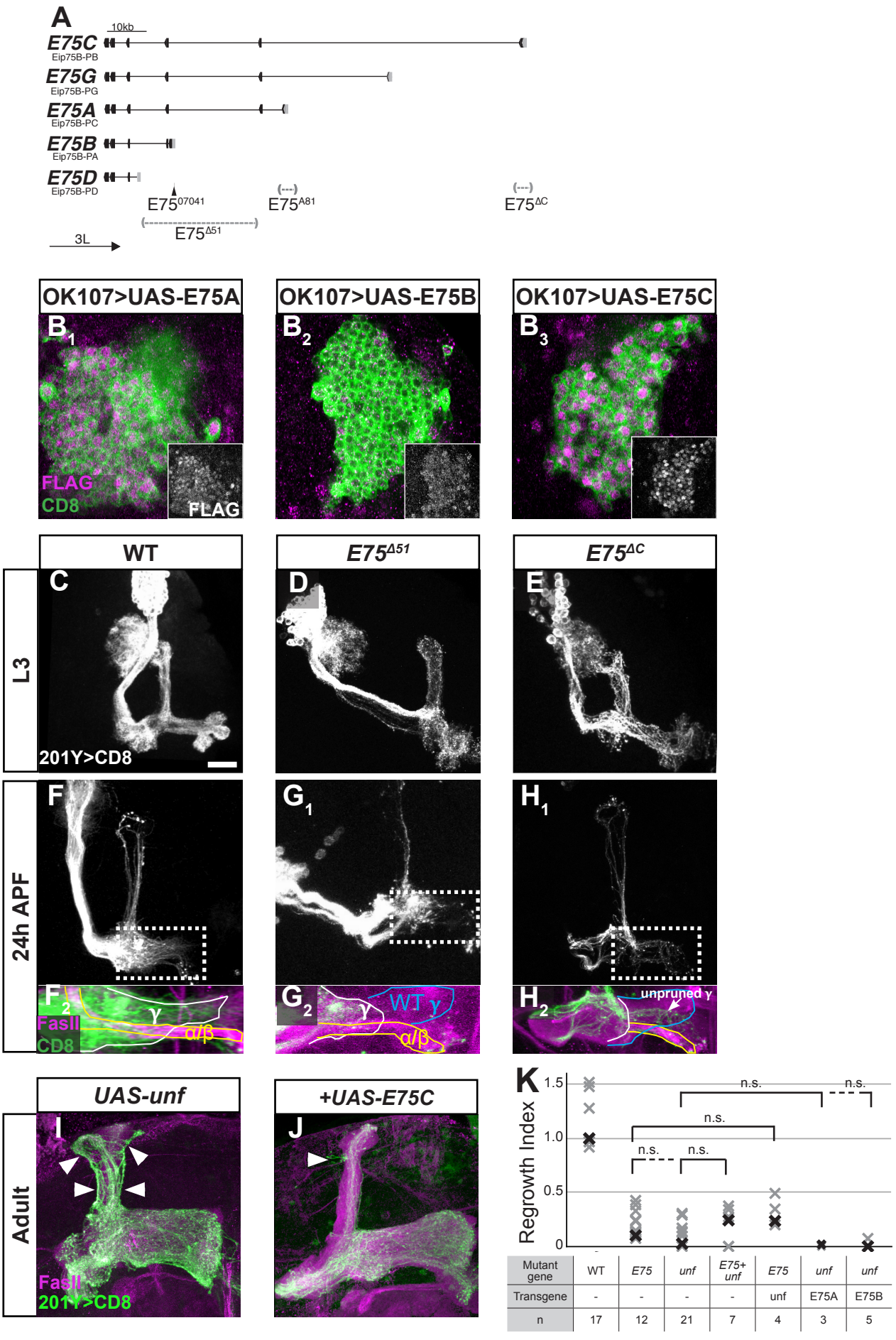

Rabinovich et al Figure S2

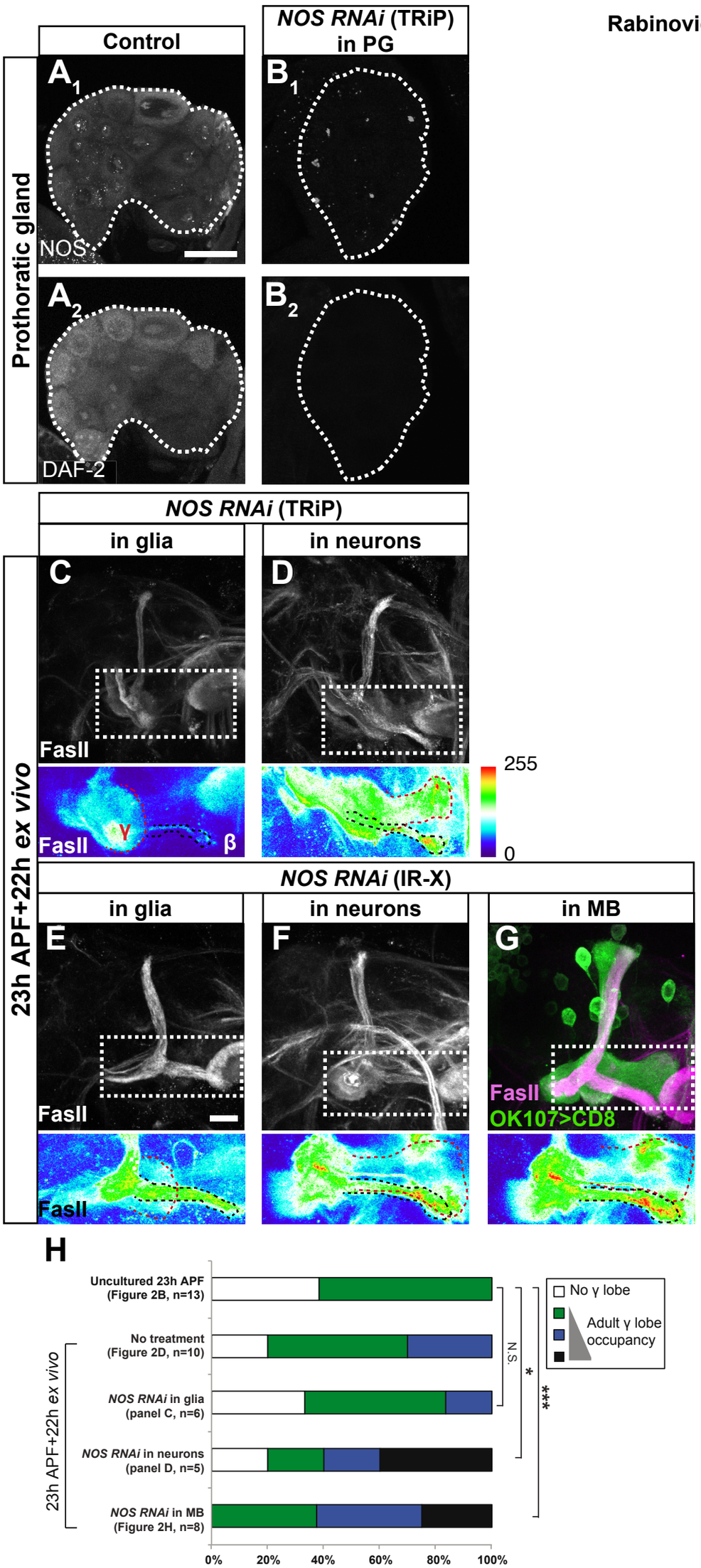

Rabinovich et al Figure S3

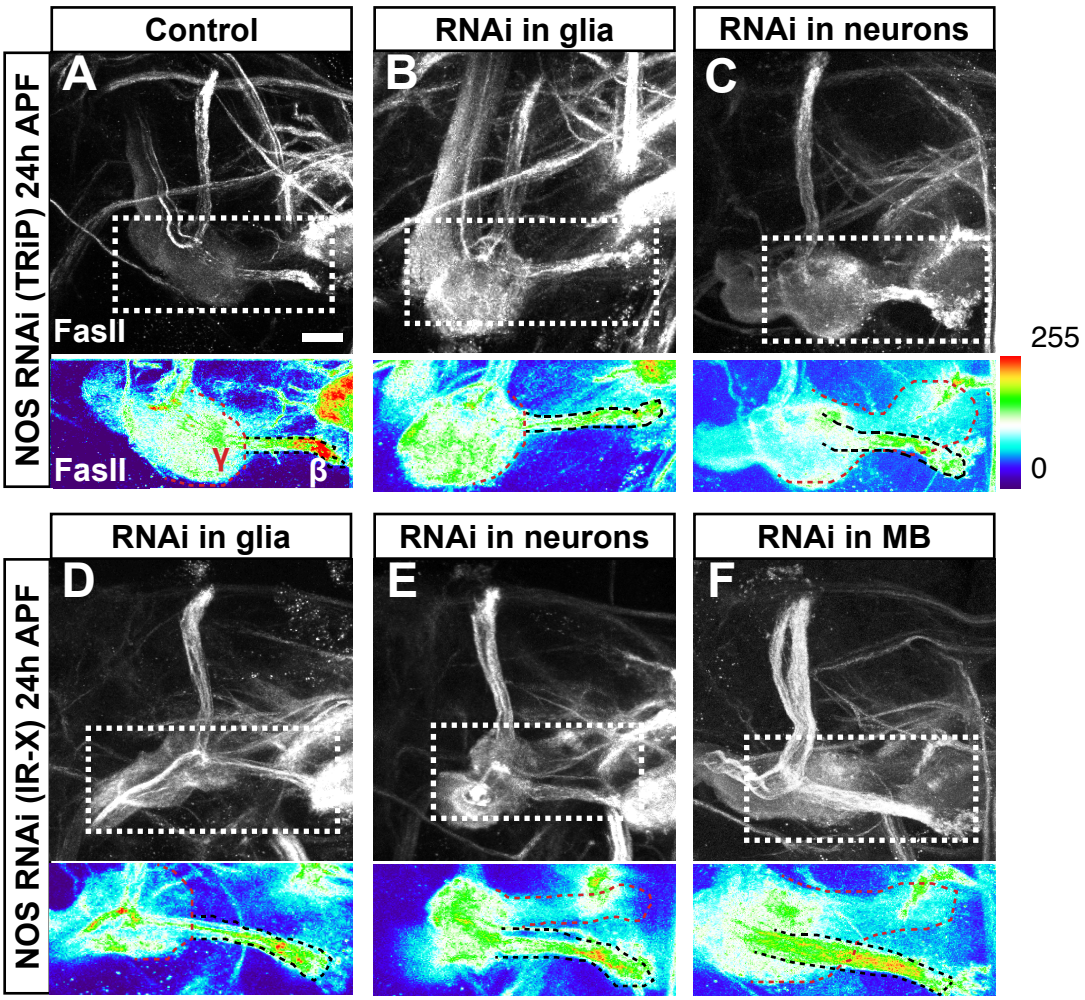

Rabinovich et al Figure S4

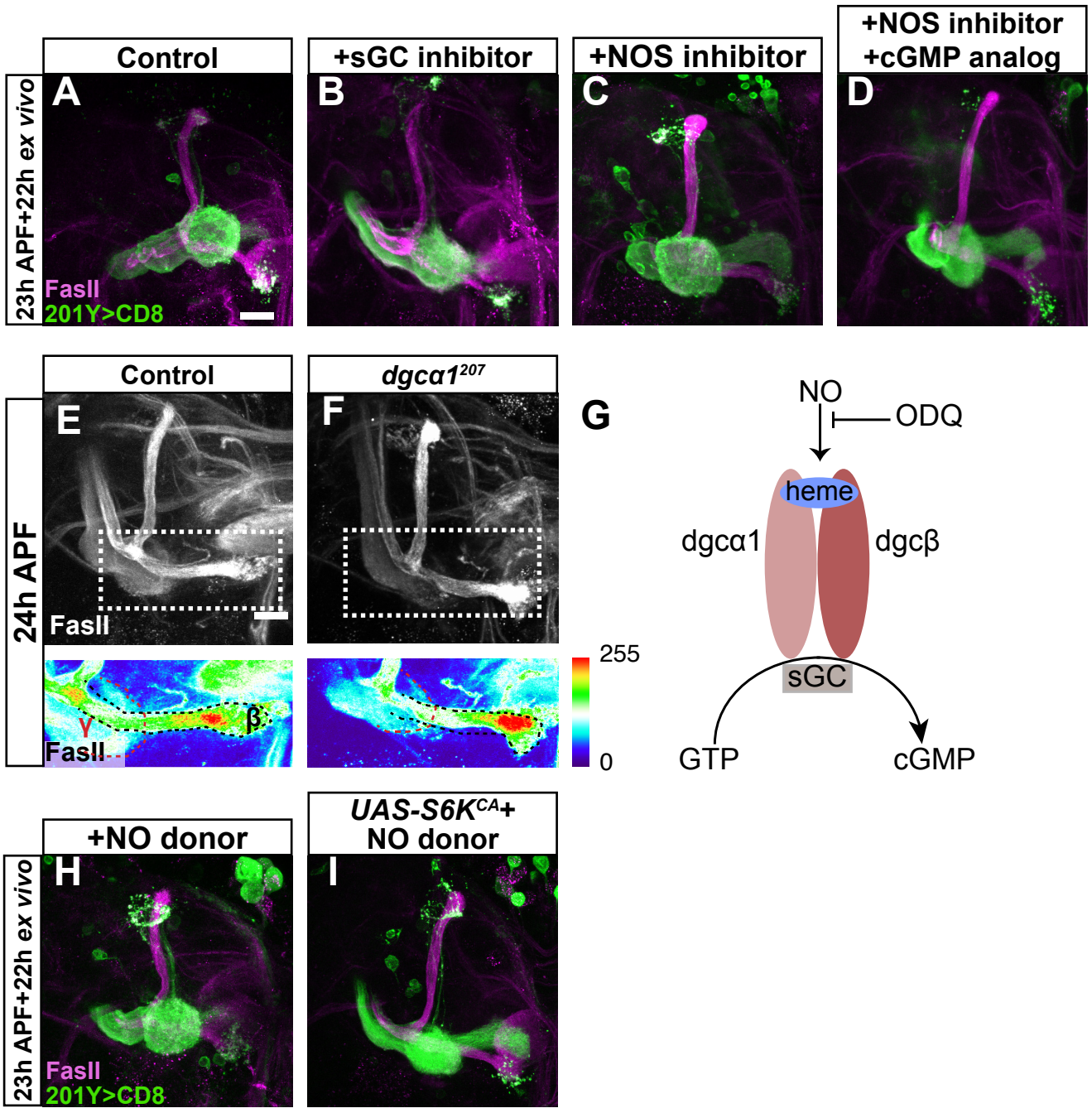

Rabinovich et al Figure S5

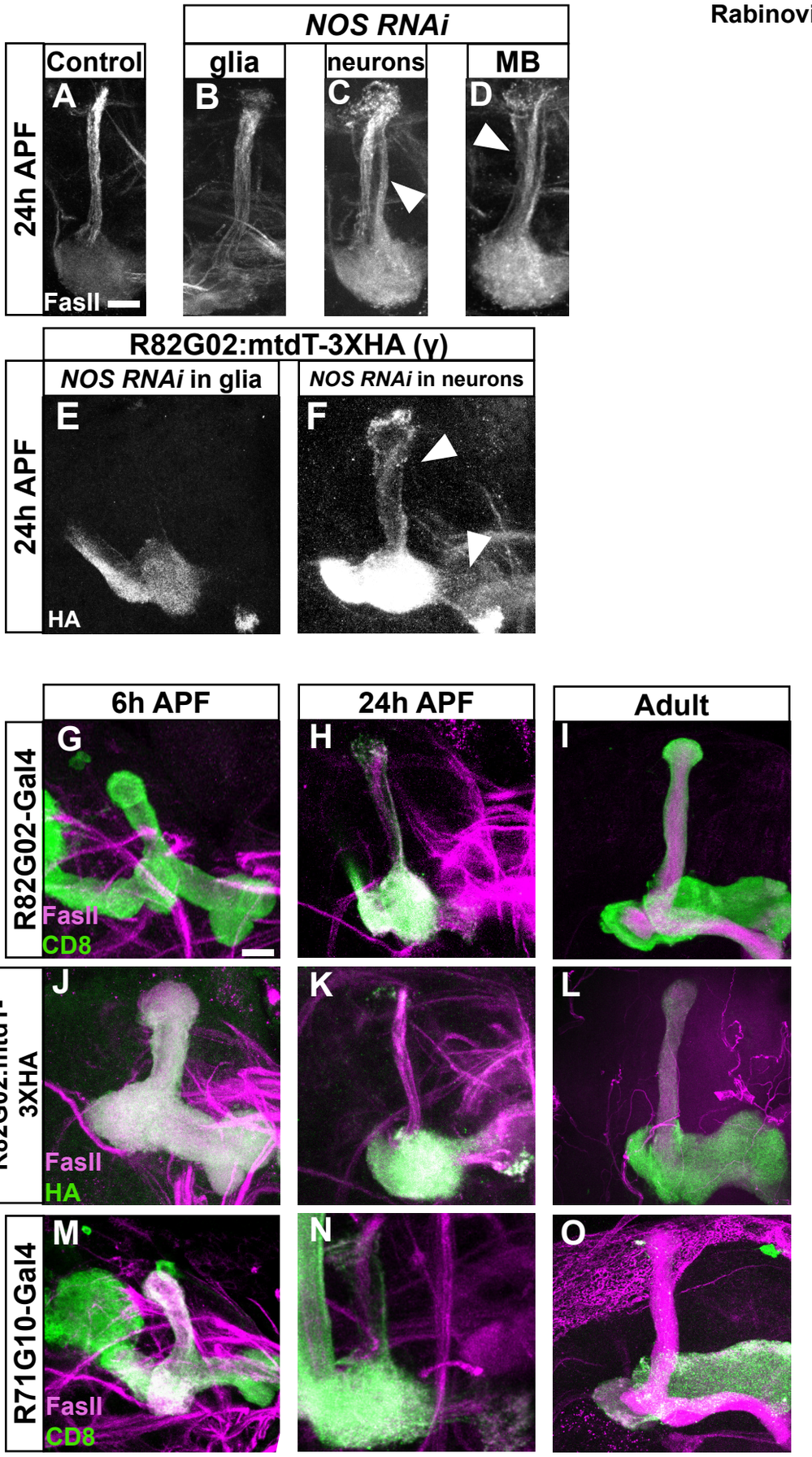

Rabinovich et al Figure S6

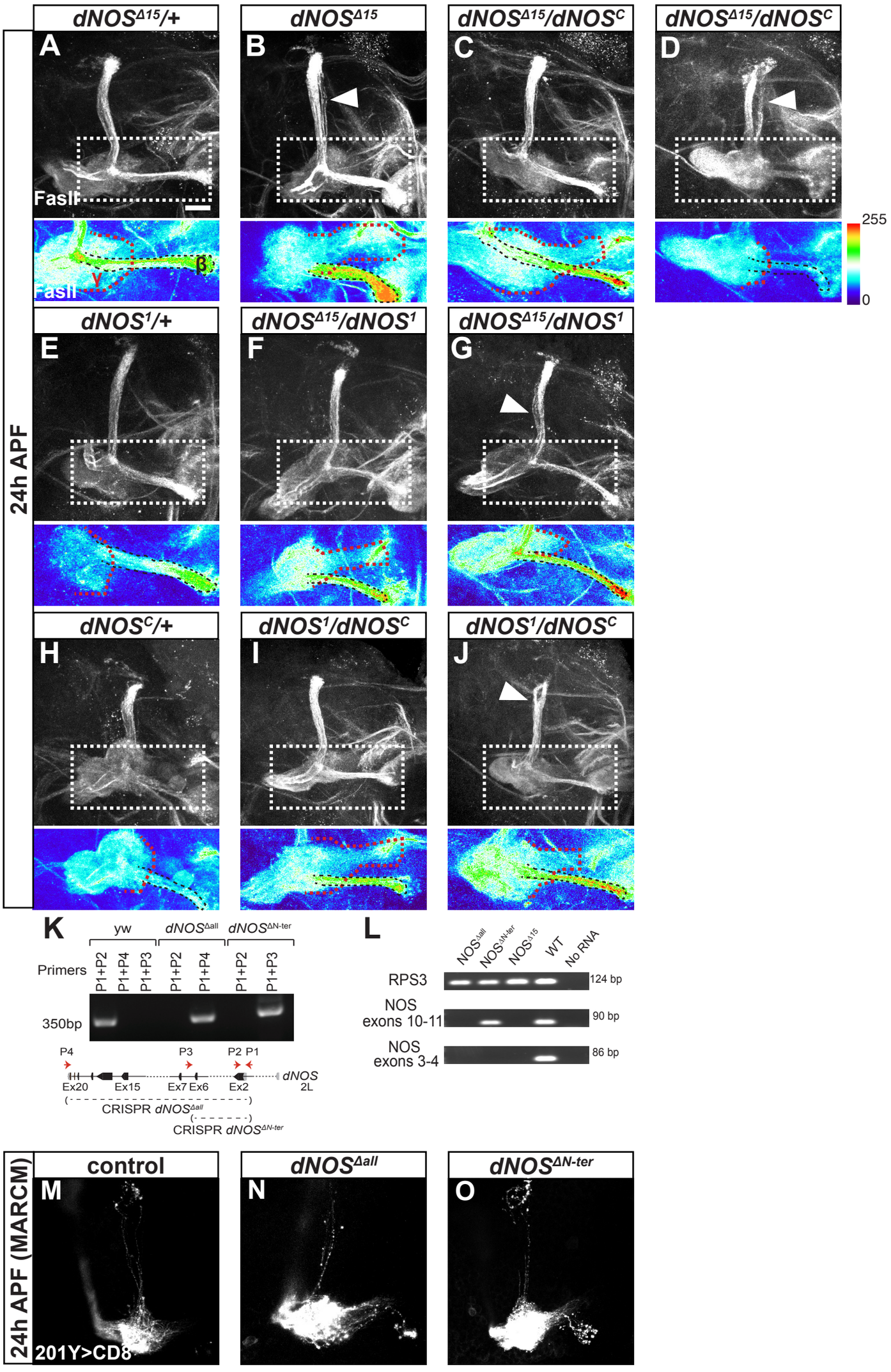

Rabinovich et al Figure S7